Journal of Peptide Science
J. Pept. Sci. 2008; **14**: 251–260
Published online 21 September 2007 in Wiley InterScience (www.interscience.wiley.com). DOI: 10.1002/psc.914

JOURNAL OF PEPTIDE SCIENCE

Structural and functional characterization of the porcine proline–rich antifungal peptide SP-B isolated from salivary gland granules

T. CABRAS,[a] R. LONGHI,[b] F. SECUNDO,[b] G. NOCCA,[c] S. CONTI,[d] L. POLONELLI,[d] C. FANALI,[c] R. INZITARI,[c] R. PETRUZZELLI,[e] I. MESSANA,[a] M. CASTAGNOLA[c] and A. VITALI[f]*

[a] Department of Sciences Applied to Biosystems, University of Cagliari, Cittadella Universitaria, Monserrato I-09042, Cagliari, Italy
[b] Institute for the Chemistry of Molecular Recognition, National Research Council (C.N.R.), Sez. Milano, via Mario Bianco 9, Milano, Italy
[c] Institute of Biochemistry and Clinical Biochemistry, Faculty of Medicine, Catholic University, Largo F. Vito 1, Rome I-00168, Italy
[d] Department of Pathology and Laboratory Medicine, University of Parma, V. Gramsci 14, 43100 Parma, Italy
[e] Department of Biomedical Sciences, University 'G. D'Annunzio' Via dei Vestini, 31, 66100 Chieti Scalo (CH), Italy
[f] Institute for the Chemistry of Molecular Recognition, National Research Council (C.N.R.), Sez. Roma, L.go F. Vito 1, 00168 Roma, Italy

Received 23 March 2007; *Revised 26 June 2007*; *Accepted 6 July 2007*

Abstract: A 1905-Da cationic proline-rich peptide, named SP-B, was recently isolated by our group as the main component of salivary gland granules, and its primary sequence fully characterized by means of automated Edman sequencing and LC-MS/MS tools. In the present study SP-B is shown to possess antifungal activity when challenged with strains of *Cryptococcus neoformans*, *Candida albicans* and *Aspergillus fumigatus*, while only negligible antibacterial activity was detected. Furthermore, SP-B was found to be non-cytotoxic when tested on fibroblast cell lines. To obtain information regarding its structure affinity, capillary electrophoresis (CE), circular dichroism (CD) and attenuated total reflection (ATR)-FT/IR experiments were performed. CE revealed a pH dependence of the hydrodynamic radial dimensions both in aqueous and 2,2,2-trifluoroethanol solutions. CD and ATR-FT/IR measurements confirmed the structure–pH relationship, revealing a secondary structure composed of mixed proportions of polyproline-II, unordered and turn motifs, the last being more evident in the zwitterionic form of the peptide. From these findings SP-B peptide could be classified as a new member of the proline-rich antimicrobial peptide family. Copyright © 2007 European Peptide Society and John Wiley & Sons, Ltd.

Keywords: proline-rich peptides; antifungal; circular dichroism; FT-IR; capillary electrophoresis; *Cryptococcus neoformans*

INTRODUCTION

Proline-rich peptides (PRPs) have acquired considerable interest in the past years owing to the wide variety of their biological activities. The definition proline-rich generally refers to peptides whose primary structure is composed of more than 30% proline residues [1]. Some PRPs constitute a large group of linear peptides related to innate immunity, characterized by a high content (up to 50%) of proline residues [2]. Most of the known antimicrobial PRPs have been isolated from insects, showing similar motif patterns and amino acid sequences [3]. The *Drosophila melanogaster* antibacterial arsenal is composed of seven distinct groups of peptides, each of them having a specific antimicrobial activity [4]. A large family of PRPs is represented by drosocins isolated from Hymenoptera, Lepidoptera, Hemiptera and Diptera [5]. Two peculiar features are characteristic of these peptides, which are represented by the presence of repeated Pro-Arg-Pro tripeptide motifs and by the glycosylation of a threonine residue located in the middle of the chain. Apidaecines are another group of PRPs derived from the *Apis* genus [6]. These are 18–20-residues-long peptides bearing a highly conserved sequence located at the *C*-terminal region represented by either a Pro-Arg-Pro or a Pro-His-Pro-Arg-Ile/Leu motif. Pyrrhocoricins are a well-known group of peptides [7] that share similar characteristics with drosocins and apicidins, such as *O*-threonine glycosylation and the presence of PRP sequence repeats. In many cases it has been recognized that insect proline-rich antibacterial peptide activity is due to small variable regions that affect the species-specificity features of these molecules. Antibacterial proline and arginine-rich peptides have been also isolated from mammals and are classified in the cathelecidins and bactenecins families [8,9]. The best-known member of the cathelecidins family is the PR39 proline–arginine-rich peptide isolated from pig intestine [10]. This is a multi-functional peptide because it exerts antimicrobial activity against *Escherichia coli* and *Bacillus megaterium* [11] and inhibits NADPH oxidase [12] and caspase activities [13]. The bactenicin group comprehends the Bac5 and Bac7 peptides isolated from bovine neutrophils [14] sharing a high similarity (75%) with PR-39 [15]. They exert antimicrobial activity especially against

*Correspondence to: A. Vitali, Institute for the Chemistry of Molecular Recognition, National Research Council (C.N.R.), Sez. Roma, L.go F. Vito 1, 00168 Roma, Italy; e-mail: alberto.vitali@icrm.cnr.it

Gram-negative bacteria, but also act as antiviral agents against *Herpes simplex* [16]. PRPs include also those peptides implied in the interaction with the proline-rich sequence (PRS) recognition domains, which play key roles in biological processes requiring the coordinated assembly of multi-protein complexes [17,18]. Profiline, SH3, WW, EVHI, GYF, UEV and the prolyl-4-hydroxylase domain represent, up to now, the superfamily of PRS-recognition domains [19,20]. These domains are characterized by common features such as the presence of conserved aromatic amino acid residues that determine the PRP binding mechanism.

Recently, two new PRPs, named SP-A and SP-B, have been isolated by our group from pig parotid granules [21]. The sequence of SP-B, the object of this study, corresponds to APPGARPPPGPPPPGPPPPGP. This peptide accounts for more than 60% of parotid granule protein content, and a similar percentage was found in pig whole saliva [21].

The aim of this study was to elucidate the possible biological functions of this abundant, new PRP, by performing diverse biological tests. Interesting antifungal activities have been found, prompting us to carry out a structural study on SP-B combining capillary electrophoresis (CE), circular dichroism (CD) and FT/IR spectroscopy. The interest on the structural features of SP-B was also due to the very high percentage of proline residues present. The left-handed polyproline-II (PP-II) helix adopted by the majority of the PRPs seems, in fact, to be the required conformation to express antifungal activity [22].

MATERIALS AND METHODS

Synthesis and Purification of SP-B Peptide

SP-B peptide was assembled on an Applied Biosystem Peptide Synthesizer 433A (Foster City, CA, USA) on a preloaded proline-2-chlorotrityl resin (Novabiochem, Laufelfingen, CH) following the Fmoc protocol for step-wise SPPS [23,24]. Fmoc amino acids were from Novabiochem. All couplings were carried out with five-fold excess of activated amino acid in the presence of 10 equivalents of *N*-ethyldiisopropyl amine, using *N*-[(dimethylamino)-1-*H*-1,2,3-triazole-[4,5-b]pyridine-1-ylmethylene]-*N*-methylmethanaminium hexafluorophosphate *N*-oxide (HATU, PE Biosystems, Inc., Warrington, UK) as activating agent for the carboxy group. At the end of peptide chain assembly, the peptide was cleaved from the resin by treatment with a mixture of 80% trifluoroacetic acid, 5% water, 5% phenol, 5% thioanisole, 2.5% ethandithiol and 2.5% triisopropylsilane for 3 h at room temperature, with concomitant side-chain deprotection. The resin was filtered and the peptide was precipitated in cold *tert*-butylmethyl ether. After centrifugation and washing with *tert*-butylmethyl ether, the peptide was suspended in 5% aqueous acetic acid and lyophilized.

Analytical and semi-preparative reversed-phase high-performance liquid chromatography (RP-HPLC) was carried out on a Tri Rotar-VI HPLC system equipped with a MD-910 multi-channel detector for analytical purposes or with a Uvidec-100-VI variable UV detector for preparative purpose (all from JASCO, Tokyo, Japan). Analytical RP-HPLC was performed on a Jupiter 5 μ C18 300 A column (150 × 4.6 mm, Phenomenex, Torrance CA, USA). Semi-preparative RP-HPLC was performed on a Jupiter 10 μ C18 300A (250 × 21.2 mm, Phenomenex, Torrance CA, USA). Linear gradients of acetonitrile in water/0.1% TFA (v/v) were used to elute the bound peptide.

Matrix-assisted laser desorption/ionization time-of-flight (MALDI-TOF) mass spectrometric analysis were performed on a Autoflex workstation (Bruker Daltonics, Bremen, DE). α-Cyano-hydroxy cinnamic acid (HCCA) was employed as the matrix.

Biological Tests and *In Vitro* Evaluation of Fungicidal Activity

The fungicidal activity *in vitro* was assessed by colony forming unit (CFU) assays as previously described [25]. Fungi to be tested (*Candida albicans* UP10, *Cryptococcus neoformans* AIDS 25 and *Aspergillus fumigatus* UP1) were grown in Sabouraud dextrose agar plates at 30 °C for 24–48 h (yeasts) or 4–5 days (*A. fumigatus*). Yeast cells and conidia were suspended in sterile distilled water ($3–5 \times 10^4$ cells/ml), and 10 μl of the suspension was added to 90 μl of H_2O containing the synthetic peptide at different concentrations (105–1.6 μM). H_2O alone served as control. After incubation for 6 h (yeasts) or 18 h (*A. fumigatus*) at 37 °C with the respective reagents, the fungal cells were dispensed and streaked on the surface of Sabouraud agar plates, which were then incubated at 30 °C, and colonies were enumerated after 48–72 h. Each experiment was performed in triplicate. Peptide fungicidal activity was determined as the percentage of CFU inhibition, according to the formula: (100 − (CFU experimental group/CFU control) × 100). Peptide median effective concentration (EC_{50}) was calculated by non-linear regression analysis using Graph Pad Prism 4.01 software.

Cells and Treatments

Mouse 3T3-fibroblasts (Swiss albino mouse cell line) (Istituto Zooprofilattico, Brescia, Italy), human tumoral melanocytes (MEWO) and HL-60 were grown in a 5% CO_2 atmosphere at 37 °C in Dulbecco's Modified Eagle Medium (DMEM) with Hepes (10 mM), glucose (1.0 g/l), $NaHCO_3$ (3.7 g/l), penicillin (100 units/ml), streptomycin (100 μg/ml) and 10% FCS (fetal calf serum).

Human granulocytes were isolated from peripheral blood. The isolation procedure was the following: a physiological solution (PS) was added in 1 : 1 ratio to 5 ml of blood. Red cells were left to precipitate for 30 min, upon treatment with 6% (w/v) of Destane. Plasma was centrifuged at 1200 *g* for 40 min at 20 °C, and the resulting pellet containing granulocytes was suspended with 2 ml of PS, 6 ml of water and 2 ml of a 3.6% (w/v) NaCl solution. After several washings, granulocytes were aliquoted in ratios of 1 000 000 cells/ml and incubated at 37 °C for 48 h with different SP-B peptide concentrations (2.5, 5, 10, 50 and 100 μM).

DOI: 10.1002/psc

Cytotoxicity Tests

The possible cytotoxic effects of the SP-B peptide were studied on mouse fibroblasts 3T3-Swiss cell line using the neutral red uptake (NRU) and thiazolyl blue tetrazolium bromide (MTT) tests. In order to evaluate the cytotoxic effects of the SP-B, the lyophilized peptide was prepared at different final concentrations (2.5, 5, 10 and 50 μM) and dissolved in DMEM (2.2 ml) checking for the final pH. Fibroblasts (1×10^4) in DMEM (200 μl) were seeded in individual wells of a 96-well tissue culture plate and cultured to sub-confluent monolayer for 24 h. The cellular vitality was evaluated by NRU and MTT tests after 24, 48, 72 and 96 h after addition of the peptide at 37 °C. NRU assay was performed according to Borenfreund and Borrero [26]: a neutral red aqueous solution (0.4%) was added to each well to obtain a final concentration of 50 μg/ml and, after incubation for 4 h at 37 °C, the supernatant was discharged. The intra-cellular neutral red was mixed with a solution of 50% ethanol with 1% acetic acid (200 μl) and the optical density (OD) of the solution present in all the wells was determined using an automatic microplate photometer (Packard Spectracount, Packard BioScience Company, Meriden USA) at a wavelength of 540 nm. MTT test was performed according to Wataha *et al.* [27]: 20 μl of a 5 mg/ml solution of MTT in PBS (phosphate buffer, 0.1 M, pH 6.5) was added to the medium (200 μl) and after incubation for 4 h at 37 °C the intra-cellular formazan crystals produced were solubilized with a solution of HCl in isopropanol (4×10^{-2} M, 200 μl). The OD of the solution contained in each well was determined using the microplate photometer at a wavelength of 570 nm. Each experiment was performed in sextuplicate and the cell cytotoxicity was calculated according to Hashieh *et al.* [28].

The reactive oxygen species (ROS) metabolism of the THP-1 cell line and of the peripheral blood monocyte (PBM) was studied by a chemiluminescence technique according to De Sole *et al.* [29]. Chemiluminescence systems were composed of lucigenin (*N*,*N*′-dimethyl-9-9′-biacridinium dinitrate, 100 nmoles) or luminol (100 nmoles), cells (1×10^5) treated with all *trans* retinoic acid (ATRA)or untreated (used as control), in the presence or absence of phorbol 12-myristate 13-acetate (PMA, 1.50 nmoles) or opsonized zymosan in a final volume of 1 ml reached with modified KRP buffer. The measures were performed with an automatic luminometer (Autolumat LB 953, EG&G, Turku, Finland).

The chemiluminescence of PBM was assessed in basal condition or after stimulation of phagocytes with PMA (0.5 nmoles), in presence of lucigenin. Assays were performed in triplicates at 25 °C. The chemiluminescence parameter considered for analysis was the following treatment index (TI):

$$TI = \frac{\text{Photons signal (area) produced by treated cells}}{\text{Photons signal (area) produced by untreated cells}} \times 100$$

Capillary Electrophoresis

Synthetic SP-B peptide was used in CE experiments. The electrophoretic runs were carried out with a polyvinyl alcohol (PVA) coated capillary. The capillary length was 30 cm (20 cm at the detection window) with an i.d. of 75 μm. The applied constant voltage was 10 kV and the running temperature was set at 20 °C. The samples were usually prepared from a stock solution (0.425 mmol/l) diluted to a final concentration of 0.1 mmol/l with the suitable running buffer. Common buffers, sodium formate, pH 2.24–4.26; sodium acetate, pH 4.45–5.94; 2-(*N*-morpholino)ethanesulfonic acid (MES), pH 6.09–6.40; 3-(*N*-morpholino) propanesulfonic acid (MOPS), pH 6.94; *N*-(2-hydroxyethyl)-piperazine-*N*′-2-ethanesulfonic acid (HEPES), pH 7.43; tricine, pH 7.94; *N*-tris(hydroxymethyl)methyl-3-aminopropanesulfonic acid (TAPS), pH 8.30–8.90, *N*-cyclohexyl-3-aminopropanesulfonic acid (CAPS), pH 9.20–11.40 and sodium phosphate, pH 12.00–12.48 of constant 10 mmol/l ionic strength were prepared according to reported procedures [30] and added to 30 mmol/l NaCl to ensure a total ionic strength of 40 mmol/l. The pH of the running buffers was accurately checked by high-quality standard buffers (Merck) using two pH meters in order to ensure that measurements error would not be higher than 0.03 pH units. Acetanilide was employed as the electro-osmotic flow (EOF) marker, added to every sample to a final concentration of 0.5 mg/ml. The CE apparatus employed was a Beckman P/ACE System MDQ equipped with diode array detector and Gold Nouveau software for automated apparatus control and data acquisition. Injections, performed by pressure for 3 s, corresponded to about 11.0 nl. The reference detection absorbance wavelength was 220 nm. Mobility values were the mean of at least three measurements. Effective PRP–SP-B peptide mobility was calculated by subtracting from the observed mobility the value of the EOF, determined by the mobility of acetanilide, as reported in the following formula:

$$\mu_{\text{eff}} = L \times l/V \times (1/t_{\text{PB}} - 1/t_{\text{eof}})$$

where μ_{eff} is the effective mobility, L the total length of the capillary, l is the length of the capillary to the detection window, V is the applied voltage and t_{PB} and t_{eof} are the migration times of PRP–SP-B and of acetanilide, respectively. In order to compare mobility values determined in water and hydro-organic solutions, intrinsic mobilities (μ_{intr}) was calculated by multiplying μ_{eff} and the viscosity (η).

Intrinsic electrophoretic mobility values were analysed according to the least-squares fitting procedures utilizing a modified form of the Stokes–Einstein equation, taking into account the Stokes radius (r_i) and the molar fraction (x_i) of the ith species:

$$\mu_{\text{int } r} = \mu_{ep} \cdot \eta = \frac{q}{6\pi} \cdot \sum_{i=1}^{i=k} \frac{Z_i}{r_i} \cdot \mathrm{x}_i \qquad (1)$$

In this equation q is the electronic charge (1.60×10^{-19} coulomb), η is the viscosity of the medium (water: 8.95×10^{-4} N s m^{-2} at 20 °C; water/TFE (70 : 30, v/v): 1.38×10^{-3} N s m^{-2} at 20 °C), Z_i is the number of electrolyte elementary charges. The molar fraction is related to proton concentration and the peptide dissociation constants according to the following relationships:

$$x_i = \frac{[H^+]^{(k-i)} \cdot \beta_{(i-1)}}{\sum_{i=1}^{i=k} [H^+]^{(k-i)} \cdot \beta_{(i-1)}} \qquad (2)$$

where $\beta_{(i-1)}$ is obtained from:

$$\beta_{(i-1)} = \prod_{j=0}^{j=i-1} K_j \qquad (\beta_0 = 1) \qquad (3)$$

DOI: 10.1002/psc

Attenuated Total Reflection/FT-IR Measurements

ATR/FT-IR spectra were recorded on a Spectrum One (Perkin-Elmer) spectrophotometer equipped with an ATR accessory with a ZnSe reflection element. Spectra were recorded after 40 scans at 1 cm^{-1} resolution. The samples were dissolved in different sodium phosphate buffers (all at 10 mM) depending on the required pH. Prior to analysis, the SP-B synthetic peptide was dissolved in 20 mM HCl and subsequently freeze-dried in order to remove the residual TFA derived from peptide purification. Before peptide analysis, an open beam background spectrum of the clean crystal was recorded. Subsequently, the buffer solution spectrum was recorded followed by the peptide spectrum. The spectra of buffers were hence subtracted from those of the peptide. During measurements performed at 25 °C, the crystal was continually flushed with nitrogen to eliminate residual water vapors. Usually 1 µl of a 1 mg/ml (w/v) solution of SP-B peptide was employed for any measurement.

Circular Dichroism Measurements

CD spectra were obtained on a Jasco J-600 spectrophotometer equipped with a thermostatic temperature controller. CD spectra were recorded in a quartz cell of 0.1 cm of path length at 25 °C between 190 and 250 nm, using 2.0 nm bandwidth and scanning rate of 20 nm/min with a wavelength step of 0.1 nm and a time constant of 0.1 s. SP-B peptide was dissolved in 10 mM sodium phosphate buffers at the required pH. A TFE 30% (v/v) aqueous solution was employed when necessary. CD band intensities are expressed as molar ellipticities, ($[\theta]_M$ in deg cm^2 $dmol^{-1} \times 10^{-3}$).

Spectroscopic Data Treatment

ATR-FT/IR spectra were used to obtain the second derivative spectra with the Peak Fit 4.12 (Sea Solve Software, Inc., San Jose, CA) program. A 21% smoothing process, employing the Savitzky–Golay algorithm, was performed and the resulting peaks were used as reference for the subsequent peak-fitting analysis performed with the same program. A linear base line was employed and Gaussian peaks were produced after an iterative adjustment of data until the SSE statistical parameter was under 1×10^{-4}, indicating a good fitting analysis. The resulting peak areas of Amide I were used to determine the contribution of each secondary structure motif.

CD spectra were analysed employing the Selcon3 program available on Dichroweb web site (www.cryst.bbk.ac.uk/cdweb/html/home.html) [31]. The data were inserted as requested by the web site manager in the range between 190 and 250 nm. The obtained results satisfied the three basic selection rules: sum of secondary structure fractions was >1; each fraction was >0.025; the RMS (deviation between the reconstructed and experimental CD) was less than 0.25 $\Delta\varepsilon$, according to the software recommendation.

RESULTS AND DISCUSSION

Chemical Synthesis and Purification

The synthesis of SP-B was achieved in a rather easy way, being facilitated by the presence of the non-hindered amino acids glycine and proline: 4 glycine over 21 and 14 proline over 21 residues. After assembly via SPPS, the peptide was recovered in high yield and homogeneously from the resin. The final peptide purification carried out in an RP-HPLC system gave rise to a high-purity sample (Figure 1). The synthetic and the natural peptide samples were therefore compared to assess their structural similarity. MALDI-TOF mass spectrometry, (Figure 2) circular dichroism (Figure 3) and FT-IR (Figure 4) analyses confirmed the identity between the two samples, which allowed the use of the synthetic peptide in all the following experiments.

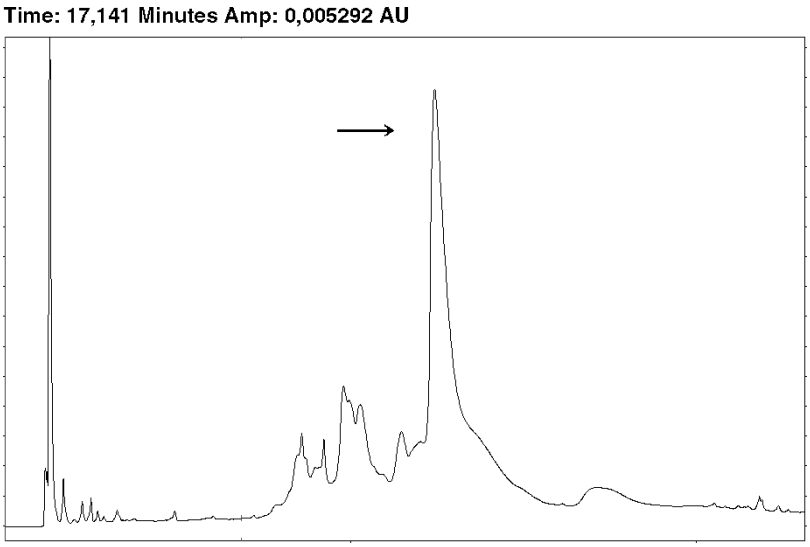

Figure 1 Preparative RP-HPLC profile of SP-B purification after solid phase peptide synthesis. The chromatogram was recorded at 220 nm. The arrow indicates the peak of SP-B.

DOI: 10.1002/psc

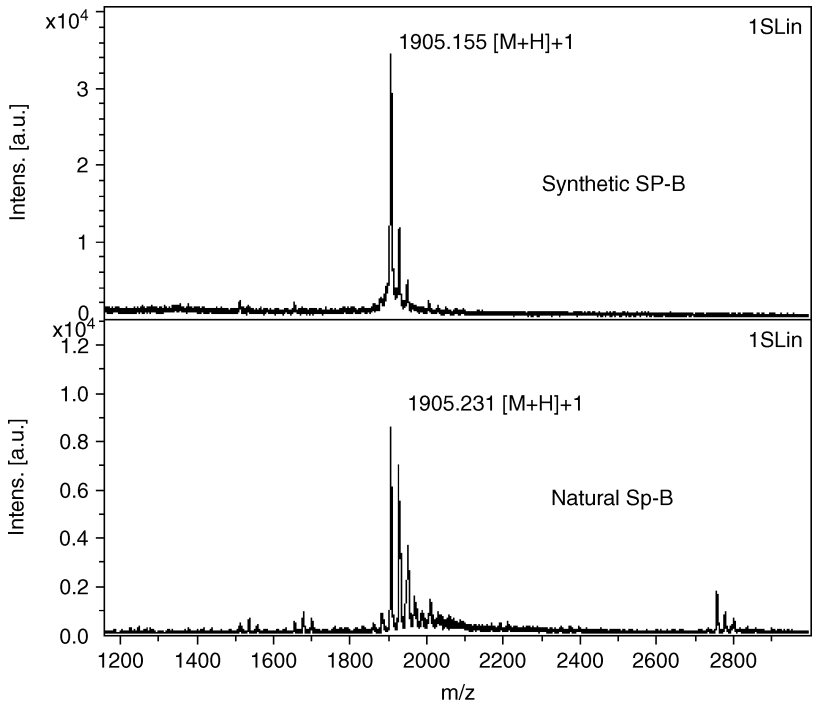

Figure 2 MALDI-ToF mass spectra of natural and synthetic SP-B peptides. The spectra were recorded employing α-cyano hydroxycinnamic acid as matrix. The natural and synthetic SP-B peptides were purified from HPLC runs before being submitted to mass analysis. The other peaks derive from Na^+ adducts.

Biological Tests

The results of the microbicidal assay of SP-B peptide against the fungal strains *C. neoformans* AIDS 25, *A. fumigatus UP1* and *Candida albicans* UP10 are shown in Figure 5. The highest growth inhibition was obtained with *C. neoformans* for which an EC_{50} value of 3.8 μM (95% confidence intervals 3.02–4.78) was found. EC_{50} values towards *Candida albicans* UP10 and *A. fumigatus* UP1 were 34.69 and 58.68 μM, respectively (95% confidence intervals 31.33–38.42 and 43.68–78.79). Concerning the antifungal activity, SP-B was more effective against *C. neoformans* and to a lesser extent against *C. albicans* and *A. fumigatus*. When it was challenged with *Pseudomonas aeruginosa* and *Staphylococcus aureus* strains, only negligible antibacterial activity was detected showing growth inhibition only at concentrations above 100 μM (data not shown). The short PRPs derived from insects and the longer mammalian relatives, such as PR-39, bactenecins and prophenins, are mostly active against Gram-negative bacteria [1]. Some of these peptides were also reported to exert antifungal activity; in particular a bactenecin-7 fragment proved to be significantly active against *C. neoformans* clinical isolates and collection strains [32], and bactenecin-5 fragments showed a candidacidal activity similar to that of the entire molecule [33]. SP-B shows a certain structural similarity with bactenecin-5. The two peptides share a PP-II conformational arrangement (see further in the text) and a positive charge due to an Arg residue; these two characteristics were in fact found to be essential for the exploitation of an antifungal activity [33]. Moreover Bactenicin-5 and SP-B showed comparable antifungal activities in terms of fungal growth inhibition [33].

SP-B was tested for other potential activities. Granulocytes derived from peripheral human blood were tested in the presence of different concentrations of SP-B in order to examine whether this peptide had functional analogy to the PR-39 peptide in the modulation of the oxidative burst process of these

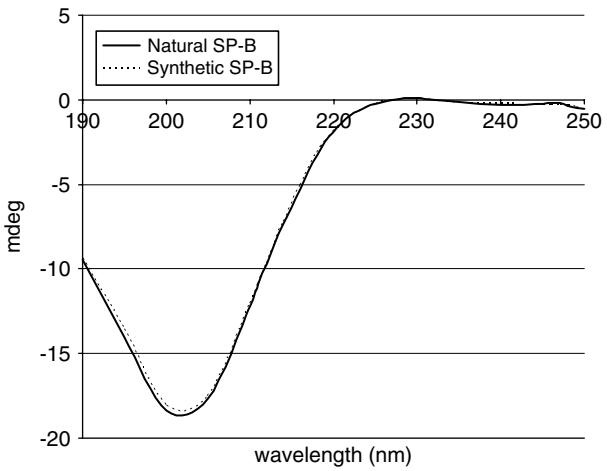

Figure 3 Far UV-CD spectra of natural and synthetic SP-B peptide. The spectra were recorded at pH 6.0 in a 10 mM phosphate buffer.

DOI: 10.1002/psc

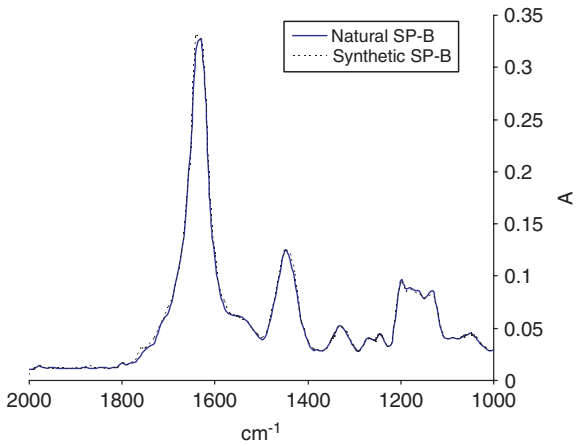

Figure 4 ATR/FT-IR spectra of synthetic and natural SP-B. The spectra were recorded at pH 6.0, in a phosphate 15 mM buffer. This figure is available in colour online at www.interscience.wiley.com/journal/jpepsci.

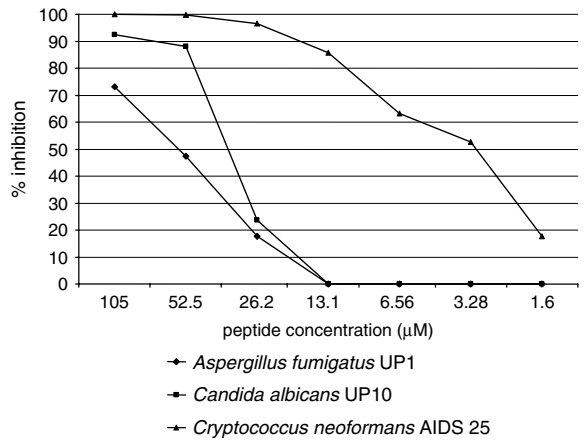

Figure 5 *In vitro* fungicidal activity of the peptide SP-B (Q95JC9) against fungal strains of three different species.

cells [12]. SP-B peptide was also tested on the HL-60 cell line in order to examine a possible role in the proliferation rate or in modulating the differentiation process in granulocytes, both in the presence and in the absence of ATRA. In all the above-mentioned tests, SP-B did not show any activity; moreover SP-B peptide was found to be non-cytotoxic when tested on 3T3 Swiss and MEWO cell lines using NRU and MTT tests, indicating the absence of membrane damage deriving from an interaction with the peptide. This is typical for certain antimicrobial PRPs, as their structure arrangement promoted by proline residues permits the entry in the lipid membrane bi-layer, and the subsequent interaction with a specific target inside the cell [2,34].

Structural Studies

The interesting biological activity of SP-B prompted us to determine the structural features of this peptide employing different analytic techniques.

CE was employed in order to determine p*K*a and Stokes radius values of PRP–SP-B in aqueous solution and in 2,2,2-trifluoroethanol (TFE)/water mixtures. Electrophoretic mobility (μ) was measured in the pH range 2.24–12.48 in water and 2.24–12.00 in TFE/water (30 : 70 v/v) using buffers at constant ionic strength. The use of a TFE/water (30 : 70 v/v) solvent system was chosen in order to create a cell-membrane-like environment [35,36].

The intrinsic mobility values (μ_{intr}) were analyzed according to non-linear least-squares fitting procedures utilizing the modified Stokes-Einstein equation (Eqn (1)) previously reported [37]. The analysis permitted determination of peptide proton dissociation constants and Stokes radii, which are reported in Tables 1 and 2. The continuous curves of Figure 6 represent the theoretical μ_{intr} calculated from these values. In aqueous solution the curve is characterized by three plateau around pH 2.0, 6.0 and 10.5, corresponding to the presence of high percentages of the peptide forms with a net charge of +2, +1 and 0, respectively. A solution showing a high percentage of the peptide form with a net charge of −1 could not be obtained under our experimental conditions, because it is predominant outside the pH range investigated (below pH 12.0). The charged forms derive from three ionizable amino acid residues: the *N*-terminal Ala-1, the *C*-terminal Pro-21 and the Arg-6 residue. Even though the exact p*K*a of the arginine residue was not determinable, the curve clearly shows that its value must be over 12.5. Interestingly, the Stokes radius of the charged form +1 obtained from the fitting procedure (r_i parameter) showed a decrease of about 3 Å (from 26.2 to 23.5 Å) with respect to the +2 form, implying that a significant peptide structural change occurs around pH 4.00. In H_2O/TFE (70 : 30 v/v) mixtures the opposite situation was observed, with an increase of the Stokes radius of about 5 Å (from 24.3 Å to 29.2 Å) around the same pH. As observed with other peptides, SP-B structural arrangement is pH dependent [38,39] and can be explained to be due to the attraction between the charged side chains and/or the terminal groups [40]. The pH-dependent strong decrease of Stokes radius of SP-B observed in aqueous solution is in fact connected to the deprotonation of the *C*-terminal Pro-21 residue. A Coulumbian attraction to the Arg-6 residue could provide a transition towards a more compact structure, where some polar residues are partly excluded from water interaction. This structural transition due to deprotonation is further confirmed by the results obtained in TFE/water solutions, where the exposure of apolar external residues increases the interaction with trifluoroethanol molecules as the *C*-terminal is deprotonated. This leads to a concomitant change in the Stokes radius, opposite to that observed in aqueous solutions.

DOI: 10.1002/psc

Table 1 Ionization state and relative p*K*a's of the residues *N*-terminus, Arg-6 and *C*-terminus of SP-B peptide

Ionizable amino acids	pKa aqueous	p*K*a app TFE 30%
N-terminus	8.0 ± 0.2	7.9 ± 0.2
Arg-6	>12.5	>12.5
C-terminus	3.9 ± 0.2	3.7 ± 0.2

Table 2 Ionization states and relative Stokes radii of the synthetic peptide SP-B

SP-B charge	SP-B Stokes radius (Å)	
	Buffer	Buffer/TFE 70 : 30 (v/v)
+2 (pH < 4.0)	26.2 ± 0.2	24.3 ± 0.2
+1 (pH > 4.0)	23.5 ± 0.2	29.2 ± 0.2

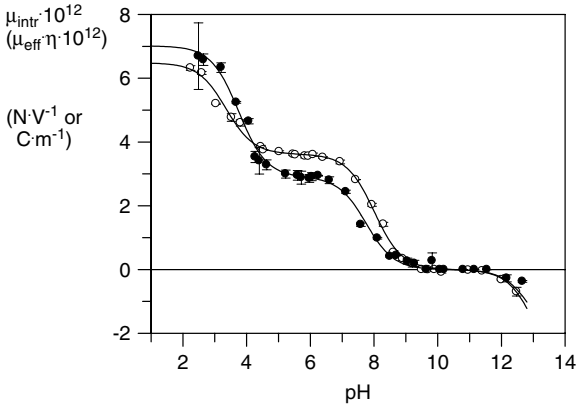

Figure 6 Electrophoretic mobility (μ) of PRP-SP-B determined in aqueous solution and TFE/H_2O mixtures at different pH_{app} values. The continuous thick curve was obtained by analysing the experimental data by least-squares best fitting procedure according to Eqn (1). (Open circles aqueous buffer, black circles TFE).

In order to obtain information about the SP-B peptide secondary structure arrangement, both CD and ATR-FT/IR experiments were performed. The spectroscopic signals in the IR bands derive from ν(C=O), δ(N–H) and ν(C–N) vibrations, while the CD data arise from electronic transitions; these two spectroscopic methods give different and independent structural information, making a data comparison not always straight-forward. In fact, while CD measurements give more accurate estimations of the α-helix content, IR is more sensitive to β-sheets and β-turn structures, but at the same time these techniques complement each other.

CD measurements were performed in phosphate buffers at pH 2.1, 6.2 and 11.0, both in phosphate buffers and in buffers/TFE (70 : 30 v/v) (Figure 7(a) and (b), respectively) in order to compare the experiments performed by CE.

In all the recorded spectra the peptide exhibited a negative π–π^* band around 202 nm ($[\theta]_M = -25 \times 10^3$ deg cm^2 dmol^{-1}) with only small variations in the θ–values of this band with pH changes. At the same time the pH increase is associated with a deviation of the curve profile between 190 and 195 nm (Figure 7(a)). A similar deviation from the classical PP-II profile was also observed by Schweitzer-Stenner *et al.* for a tri-proline peptide in its zwitterionic form [41].

The addition of trifluoroethanol at a 30% (v/v) final concentration did not modify the CD spectra profiles obtained in any of the pH conditions (Figure 7(b)), suggesting a substantial tendency of SP-B to maintain its structural arrangement in different solvent conditions.

A typical CD spectrum profile of a PP-II helix is characterized by a strong signal at 202 nm and by a positive band at 224 nm [42]. In the SP-B CD spectra a negative band at 202 nm is observed, but with minor amplitude with respect to a canonical PP-II helix, while the positive band at 224 is absent. This last observation can be explained by considering that a percentage of random-coil motif could 'disturb' the complete formation of a polyproline-II helix, contributing in this way to an unstructured arrangement of SP-B; at the same

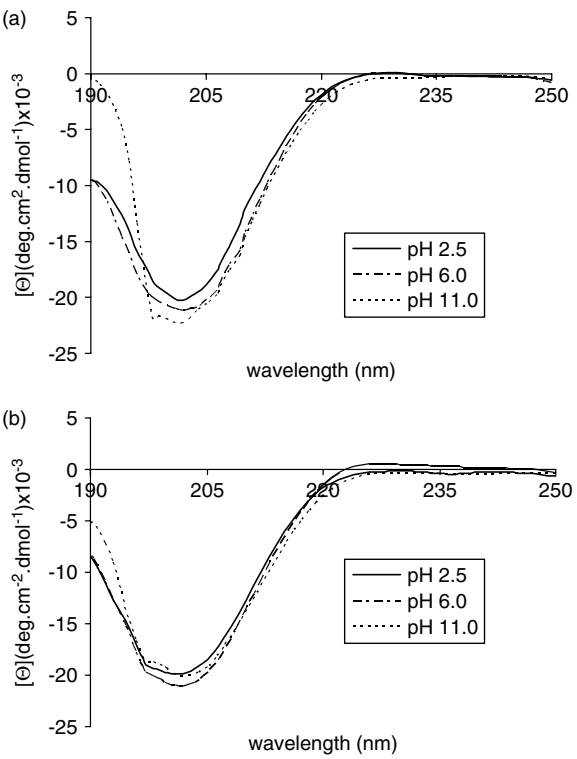

Figure 7 Far-UV circular dichroism spectra of SP-B obtained at different pHs in 10 mM phosphate buffer (a) and in buffer: TFE 70/30 (v/v) (b).

DOI: 10.1002/psc

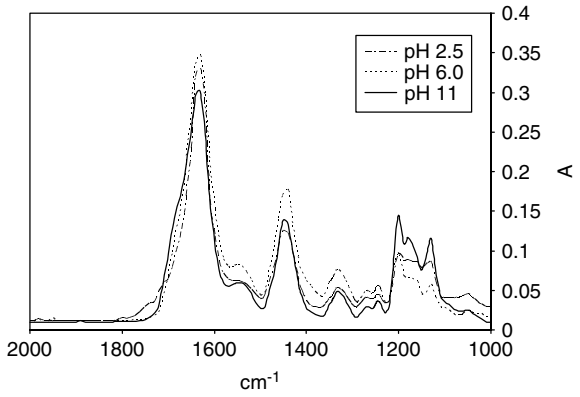

Figure 8 Superimposed spectra of peptide SP-B at pH 2.5 (dotted line), pH 6.0 (semi-dotted) and pH 11.0 (continuous line) in the 2000–1200 cm^{-1} range. Samples (0.1 mg/ml) were suspended in 10 mM sodium phosphate buffers. Curves were obtained after subtraction of the buffer signals from the peptide spectra.

time the presence of a negative band at 224 nm can be interpreted to be due to a β-turn motif contribution [43].

ATR-FT/IR studies were performed under the same conditions as employed in the CD experiments. Spectra were recorded in 10 mM sodium phosphate buffers at pH 2.5, 6.0 and 11.0 (Figure 8). Two major bands, the Amide I at 1633 cm^{-1}, and a band at 1444 cm^{-1} characterized the spectra. Other minor bands were detected at 1540–1545 (Amide II) and 1328 cm^{-1} and weaker bands were identified at 1268 and 1243 cm^{-1} (Amide III). The strong band around 1444 cm^{-1} was assigned to the proline side-chain signals, due to the contribution from CN stretching and CH_2 in-plane bending vibration [44]. The strong intensity of this band has to be ascribed to the high percentage (67%) of proline residues present in the SP-B peptide. The same spectra recorded in buffers/TFE (70 : 30 v/v) at different pH's were almost identical to each other and to those depicted in Figure 8 (data not shown), in fair agreement with the data obtained from CD. It is known that the Amide I band is a good indicator of the secondary structure of a protein [45], and so we calculated the second derivative and undertook curve-fitting analysis of the Amide I band (1700–1600 cm^{-1}) in order to estimate the contribution of the various component to the secondary structure of the SP-B peptide (Figure 9(a–c)). By this method the five main bands listed in Table 3 were detected. The absorption bands around 1620 and 1632 cm^{-1} are generally assigned to β-strand structures [45], but such a signal can be also referred to extended left-handed polyproline helices [43,46]. The bands between 1647 and 1650 cm^{-1} were assigned to unordered structures, while the bands around 1665 and 1682 cm^{-1} were assigned to β-turns. The intensity of these signals is enhanced at pH 6.0 and mostly at pH 11.0, indicating a modification in the conformational arrangement of SP-B as a function of pH change. The pH-dependent increase in turn motifs could reflect a reduction in the hydrodynamic radius, in agreement with the CE data. The data derived from FT/IR and CD experiments gave an almost converging description of the structural arrangement of SP-B peptide. CD spectroscopy is unable to quantify the exact proportion between unordered and polyproline-II helix since the PP-II motif energetically falls in the same conformational region occupied by the unordered structures [47]. In addition, unordered segments, when present together with extended polypro-II helices, do not alter the typical PP-II CD spectra profile, making the quantification of such structures uncertain [48]. FT/IR spectroscopy is helpful in this case because PP-II and unordered structures signals could be distinguished, the first being recognized by values around 1632 cm^{-1} and the second by values ranging from 1640 to 1650 cm^{-1}. The occurrence of a PP-II is suggested by the presence of PPP/PPPP motifs repeatedly found along the SP-B sequence known to strongly induce a PP-II conformational structure [49,50] in small peptides. The ARPPP segment 6–10 is also likely to form PP-II since alanine and arginine are considered inducers of a such a motif especially when followed by proline residues [51]. The following 11–21 segment is characterized by the repetitive GPPPPGPPPPGP sequence. Glycine itself

Table 3 Analysis of Amide I bands

pH 2.5			pH 6.0			pH 11.0		
Band position (cm^{-1})	Signal assignment	%	Band position (cm^{-1})	Signal assignment	%	Band position (cm^{-1})	Signal assignment	%
1616	Polypro-II	55	1620	Polypro-II	54	1619	Polypro-II	52
1632			1635			1633		
1648	Unordered	25	1650	Unordered	25	1647	Unordered	24
1665	Turns	20	1667	Turns	21	1664	Turns	24
1684			1682			1682		

DOI: 10.1002/psc

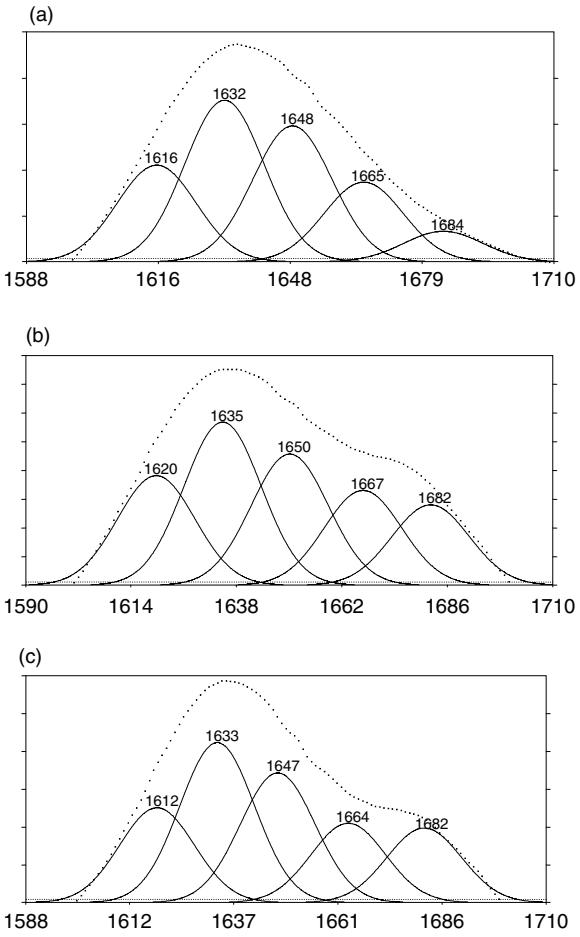

Figure 9 Curve-fitted Amide I (1700–1600 cm^{-1}) band of SP-B peptide at different pHs: (a) pH 2.5; (b) pH 6.0; and (c) pH 11.0.

does not have a good propensity for a PP-II helix, and this segment may be a mixture of PP-II/unordered structures due to the ability of glycine to function as a polypeptide chain hinge.

Amide I curve-fitting analysis shows that as the pH is increased a transition in the secondary structure from a predominance of PP-II and unordered to turn motifs occurs.

The structural arrangement of SP-B could be explained as the coexistence of random-coil and PP-II motifs as reported from CD and FT/IR data; in fact their aspect do not completely resemble either a random-coil or a PP-II typical profile. A multi-conformational equilibrium in aqueous and in water–solvent solutions of different proportions of unordered, PP-II structures and minor proportions of turns may be explained by the close proximity of the respective dihedral angle values known for these structures [52].

CONCLUSIONS

The synthesis of SP-B, a porcine salivary peptide representing the main component of parotid salivary pattern [21], and its biological and structural features are presented. SP-B shows antifungal activity, and therefore a defensive role could be postulated for this peptide. Other roles such as oral mucosa protection or tannins sequestering activities should not to be avoided; in particular, the latter has been demonstrated in human basic salivary PRPs, which predominantly show a random-coil structure [53]. The lack of a cytotoxicity against granulocytes and the remarkable antifungal activity should lead to future studies on the mechanisms by which antifungal activity is exerted by SP-B in order to ameliorate this feature for the production of new promising antifungal drugs.

Acknowledgements

The authors gratefully acknowledge Drs Lucia Di Gilio from the Institute of Biochemistry and Clinical Biochemistry, Catholic University of Rome, and Dr Domenico L. Maffei from Department of Pathology and Laboratory Medicine, University of Parma, for their helpful assistance in setting up cell cultures and biological assays. Prof. A. Bennick is also gratefully acknowledged for critically reading of the manuscript.

REFERENCES

1. Otvos L Jr. The short proline-rich antibacterial peptide family. *Cell. Mol. Life Sci.* 2002; **59**: 1138–1150.
2. Markossian KA, Zamyatnin AA, Kurganov BI. Antibacterial proline-rich oligopeptides and their target proteins. *Biochemistry (Moscow)* 2004; **69**: 1332–1344.
3. Otvos L Jr. Antibacterial peptides isolated from insects. *J. Pept. Sci.* 2000; **6**: 497–511.
4. Bulet P. *Drosphila* antimicrobial peptides. *Medicine/Sciences* 1999; **15**: 23–29.
5. Bulet P, Dimarcq JL, Hetru C, Lagueux M, Charlet M, Hegy G, Van Dorsselaer A, Hoffmann JA. A novel inducible antibacterial peptide of *Drosophila* carries an O-glycosylated substitution. *J. Biol. Chem.* 1993; **268**: 14893–14897.
6. Casteels P, Ampe C, Jacobs F, Vaeck M, Tempst P. Apidaecins: antibacterial peptides from honeybees. *EMBO J.* 1989; **8**: 2387–2391.
7. Cociancich S, Dupont A, Hegy G, Lanot R, Holder F, Hetru C, Hoffmann JA, Bulet P. Novel inducible antibacterial peptides from a hernipteran insect, the sap sucking-bug *Pyrrochoris apterus*. *Biochem. J.* 1994; **300**: 567–575.
8. Bals R, Wilson JM. Cathelicidins-a family of multifunctional antimicrobial peptides. *Cell. Mol. Life Sci.* 2003; **60**: 711–720.
9. Tokunaga Y, Niidome T, Hatakeyama T, Aoyagi H. Antibacterial activity of bactenecin-5 fragments and their interaction with phospholipid membranes. *J. Pept. Sci.* 2001; **7**: 297–304.
10. Agerberth B, Lee JY, Bergman T, Carlquist M, Boman HG, Mutt V. Aminoacid sequence of PR-39: isolation from pig intestine of a new member of the family of proline-arginine-rich antibacterial peptides. *Eur. J. Biochem.* 1991; **202**: 849–854.
11. Shi J, Ross CR, Chengappa MM, Blecha F. Identification of a proline-arginine-rich antibacterial peptide from neutrophils that is analogous to PR-39, an antibacterial peptide from the small intestine. *J. Leukoc. Biol.* 1994; **56**: 807–811.
12. Shi J, Ross CC, Leto LT, Blecha F. PR-39, a proline-rich antibacterial peptide that inhibits phagocyte NADPH oxidase

activity by binding to SRC homology 3 domains of p47 ^{phox}. *Proc. Natl. Acad. Sci. U.S.A.* 1996; **93**: 6014–6018.
13. Chan YR, Gallo RL. PR-39, a Syndecan-inducing antimicrobial peptides, binds and affects p130Cas. *J. Biol. Chem.* 1998; **273**: 28978–28985.
14. Gennaro R, Skleravaj B, Romeo D. Purification, composition, and activity of two bactenecins antibacterial peptides of bovine neutrophils. *Infect. Immun.* 1989; **57**: 3142–3146.
15. Scocchi M, Romeo D, Zanetti M. Molecular cloning of Bac-7, a proline and arginine-rich antimicrobial peptide from bovine neutrophils. *FEBS Lett.* 1994; **26**: 197–200.
16. Zerman A, Skleravaj B, Gennaro R, Romeo D. Inactivation of herpes simplex virus by protein components of bovine neutrophil granules. *Antiviral Res.* 1987; **7**: 341–352.
17. Kay BK, Williamnson MP, Sudol M. The importance of being proline: the interaction of proline-rich motifs in signalling proteins with their cognate domains. *FASEB J.* 2000; **14**: 231–241.
18. Gaczynska M, Osmulski PA, Gao Y, Post MJ, Simons M. Proline- and arginine-rich peptides constitute a novel class of allosteric inhibitors of proteasome activity. *Biochemistry* 2003; **42**: 8663–8670.
19. Cesareni G, Gimona M, Sudol M, Yaffe M. *Modular Protein Domains*. Wiley-VCH Verlag GmbH: Weinheim, 2005.
20. Gu W, Kofler M, Antes I, Freund C, Helms V. Alternative binding modes of proline-rich peptides binding to the GYF domain. *Biochemistry* 2003; **22**: 6404–6415.
21. Patamia M, Messana I, Petruzzelli R, Vitali A, Inzitari R, Cabras T, Fanali C, Scarano E, Cantucci A, Galtieri A, Castagnola M. Two proline-rich peptides from pig (Sus scrofa) salivary glands generated by pre-secretory pathway underlying the action of a proteinase cleaving Pro-Ala bonds. *Peptides* 2005; **26**: 1550–1559.
22. Antonyraj KJ, Karunakaran T, Periathamby AR. Bactericidal activity and Poly-L-proline II conformation of the tandem repeat sequence of human salivary Mucin glycoprotein (MG2). *Arch. Biochem. Biophys.* 1998; **356**: 197–206.
23. Atherton E, Sheppard RC. In *The Peptides*, vol. 9, Udenfriend S, Meienhofer J (eds.). Academic Press: San Diego, 1987; 1–39.
24. Fields GB, Noble RL. Solid phase peptide synthesis utilizing 9-fluorenylmethoxycarbonyl amino acids. *Int. J. Pept. Protein Res.* 1990; **35**: 161–214.
25. Polonelli L, Magliani W, Conti S, Bracci L, Lozzi L, Neri P, Adriani D, De Bernardis F, Cassone A. Therapeutic activity of an engineered synthetic killer antiidiotypic antibody fragment against experimental mucosal and systemic candidiasis. *Infect. Immun.* 2003; **71**: 6205–6212.
26. Borenfreund E, Borrero O. In vitro cytotoxicity assays. Potential alternatives to the Draize ocular allergy test. *Cell Biol. Toxicol.* 1984; **1**: 55–65.
27. Wataha JC, Craig RG, Hanks CT. Precision of and new methods for testing in vitro alloy cytotoxicity. *Dent. Mater.* 1992; **8**: 65–70.
28. Hashieh IA, Cosset A, Franquin JC, Camps J. In vitro cytotoxicity of one-step dentin bonding systems. *J. Endod.* 1999; **25**: 89–92.
29. De Sole P, Fresu P, Frigieri L, Pagliari G, De Simone C, Guerriero C. Effect of adherence to plastic on peripheral blood monocyte and alveolar macrophage chemiluminescence. *J. Biolumin. Chemilumin.* 1993; **8**: 153–158.
30. Gluck SJ, Steele KP, Benkö MH. Determination of acidity constants of monoprotic and diprotic acids by capillary electrophoresis. *J. Chromatogr. A* 1996; **745**: 117–125.
31. Lobley A, Whitmore L, Wallace BA. An interactive website for the analysis of protein secondary structure from circular dichroism data. *Bioinformatics* 2002; **18**: 211–212.
32. Benincasa M, Scocchi M, Podda E, Skerlavaj B, Dolzani L, Gennaro R. Antimicrobial activity of Bac7 fragments against drug-resistant clinical isolates. *Peptides* 2004; **25**: 2055–2061.
33. Raj PA, Edgerton M. Functional domain and poly-L-proline II conformation for candidicidal activity of bactenecin-5. *FEBS Lett.* 1995; **368**: 526–530.
34. Otvos L jr. Antibacterial peptides and proteins with multiple cellular targets. *J. Pept. Sci.* 2005; **11**: 697–706.
35. Castagnola M, Rossetti DV, Corda M, Pellegrini MG, Misiti F, Olianas A, Giardina B, Messana I. Predictive model for capillary electrophoretic peptide mobility in 2,2,2-trifluoroethanol-water solution. *Electrophoresis* 1998; **19**: 1728–1732.
36. Roccatano D, Colombo G, Fioroni M, Mark AE. Mechanism by which 2,2,2-trifluoroethanol/water mixtures stabilize secondary structure formation in peptides: a molecular dynamics study. *Proc. Natl. Acad. Sci.* 2002; **99**: 12179–12184.
37. Castagnola M, Rossetti DV, Inzitari R, Vitali A, Lupi A, Zuppi C, Cabras T, Fadda MB, Podda I, Petruzzelli R, Giardina B, Messana I. Capillary electrophoretic study of the binding of zinc(II) ion to bacitracin A1 in water-2,2,2-trifluoroethanol. *Electrophoresis* 2003; **24**: 1612–1619.
38. Ripoli DR, Vorobjev YN, Liwo A, Vila AJ, Scherana HA. Coupling between folding and ionization equilibria: effects of pH on the conformational preferences of polypeptides. *J. Mol. Biol.* 1996; **264**: 770–783.
39. Ramirez-Alvarado M, Blanco FJ, Serrano L. Elongation of the BH8 β-hairpin peptides: electrostatic interactions in β-hairpin formation and stability. *Protein Sci.* 2001; **10**: 1381–1392.
40. Mohanty D, Elber R, Thirumalai D, Beglov D, Roux B. Kinetics of peptide folding: computer simulations of SYPFDV and peptide variants in water. *J. Mol. Biol.* 1997; **272**: 423–442.
41. Schweitzer-Stenner R, Eker F, Perez A, Griebenow K, Cao X. Nafie LA the structure of tri-proline in water probed by polarized Raman, Fourier transform infrared, vibrational circular dichroism, and electric ultraviolet circular dichroism spectroscopy. *Biopolymers* 2003; **71**: 558–568.
42. Simon C, Pianet I, Dufourc EJ. Synthesis and circular dichroism study of the human salivary proline-rich protein IB7. *J. Pept. Sci.* 2003; **9**: 125–131.
43. Viguera AR, Arrondo JLR, Musacchio A, Saraste M, Serrano L. Characterization of the interaction of natural proline-rich peptides with five different SH3 domains. *Biochemistry* 1994; **33**: 10925–10933.
44. Barth A. The infrared absorption of amino acid side chains. *Prog. Biophys. Mol. Biol.* 2000; **74**: 141–173.
45. Singh BR. In *Infrared Analysis of Peptides and Proteins: Principles and Applications*, *ACS Symposium Series 750*, Singh BR (ed.). American Chemical Society, Symposium Series: Washington DC, 2000.
46. Lazarev YA, Grishovsky BA, Krhomova TB. Amide I band of IR spectrum and structure of collagen and related polypeptides. *Biopolymers* 1985; **24**: 1449–1478.
47. Woody RW. Circular dichroism and conformation of unordered polypeptides. *Adv. Biophys. Chem.* 1992; **2**: 37–79.
48. Sreerama N, Woody RW. Poly(pro)II helices in globular proteins: identification and circular dichroic analysis. *Biochemistry* 1994; **33**: 10022–10025.
49. Creamer TP. Left handed polyproline II helix formation is (very) locally driven. *Proteins* 1998; **33**: 218–226.
50. Sreerama N, Woody RW. A self-consistent method for the analysis of protein secondary structure from circular dichroism. *Anal. Biochem.* 1993; **209**: 32–44.
51. Stapley BJ, Creamer TP. A survey of left-handed polyproline II helices. *Protein Sci.* 1999; **8**: 587–595.
52. Bochicchio B, Tamburro AM. Polyproline-II structure in proteins: identification by chiroptical spectroscopies, stability, and functions. *Chirality* 2002; **14**: 782–792.
53. Murray NJ, Williamson MP. Conformational study of a salivary proline-rich protein repeat sequence. *Eur. J. Biochem.* 1994; **219**: 915–921.